'Modeling and Characterization of an Electrooptic Polarization controller on $LiNbO_3$', J. Lightwave technol., 1993, vol. 11, no. 7, pp. 1151–1157.

5. Chan, L.Y., Chan, C.K., Tong, D.T.K., Cheung, S.Y., Tong, F., and Chen, L.K.: 'Demonstration of data remodulation for upstream traffic in WDM access networks using injection-locked FP laser as modulator', Proc. OFC '2001, 2001, vol. 3, pp. WU5-1–WU5-3.

CMB5 **9:00 am**

Broadband Variable Optical Attenuator Based on Acousto-optic Coupling in Single-Mode Fiber

Qun Li, Tao Jin,[+] Amy A. Au, E.R. Lyons, G. Wang, Xiaoming Liu,[+] and H.P. Lee, Dept. of Electrical & Computer Engineering, University of California, Irvine CA 92697, Email: qli@ece.uci.edu; [+]Dept. of Electronic Engineering, Tsinghua University, Beijing, P.R. China, Email: xiaoming@mail.tsinghua.edu.cn

Fast tuning variable optical attenuator (VOA) is a key component for reconfigurable optical networks. At present, MEMS and free carrier absorption-based SOI waveguide p-n junction are two of the most promising approaches.[1] In this paper, we present a novel acousto-optic (AO) based VOA implemented on a single mode (SM) fiber. Compared to previous approaches, the all-fiber AO-based VOA combined the merits of all-fiber device, (low insertion loss, ease in packaging etc.) and fast response of AO-device. In addition, the devices are readily cascadable.

SM fiber acousto-optic tunable filters (AOTFs) operate on the principle of core-to-cladding modes coupling and have loss-filter like spectral characteristics. However, typical AOTFs have bandwidth of only a few nm and are inadequate for VOA application. The –3 dB bandwidth of AOTFs is determined by the length of the fiber, L and the difference in group index

$$\left(\frac{\partial\beta_c}{} - \frac{\partial\beta_{cl}}{}\right)$$

between the core and the cladding modes:[2]

$$\Delta\lambda = \frac{0.8\pi}{L\left(\frac{\partial\beta_c}{} - \frac{\partial\beta_{cl}}{}\right)}$$

In this paper, we showed that by reducing cladding diameter (by means of chemical etching) and AO interaction length, ultra-broadband AOTF can be achieved, thus demonstrating the feasibility of all-fiber AO-based VOA. The increase in filter bandwidth is due to closer match of the group index between core and cladding modes when the cladding diameter is reduced. For common step-index SM fiber, our experiment shows that the group index of core and LP_{11}^{cl} cladding modes are matched at a fiber diameter ~21 μm. Additionally, reducing cladding diameter increases the AO coupling efficiency, and hence improves the power efficiency of the device.

The experimental set up has been described in detail in Ref. 3. Fig. 1. shows the attenuation spectra of the device at different voltages with an RF frequency of 840 kHz. The length and diameter of the etched fiber (Lucent MC) are ~1.3 cm and 21 μm respectively. The bandwidth of the VOA is beyond the measurement range of the LED light source (200 nm) used in the measurement. A nearly flat attenuation spectrum over 100 nm can be maintained and be tuned from 0 to 10 dB continuously. The filtering spectrum of an unetched SM fiber is also shown in Fig. 1 for comparison. Fig. 2 shows the plot of attenuation versus RF voltage. The polarization dependent losses (PDLs) of the device at 1550 nm are 0.25 dB and 0.5 dB at an attenuation level of 6 dB and 10 dB, respectively. The total insertion loss of the device is less than 0.3 dB. The small signal modulation bandwidth of the device is greater than 50 kHz, which is in good agreement with the propagation time of the aoustic wave in the etched fiber estimated to be ~20 μs.

To increase the maximum attenuation, two identical filters are cascaded together, separated by a section of SM fiber (with plastic jacket). Fig. 3 shows the attenuation spectrum of the two-section device. Maximum attenuation up to 22 dB can be achieved while still maintaining a flat attenuation spectrum.

In summary, we demonstrated a novel, ultra-broadband (>100 nm) all-fiber AO-based VOA that with fast response time (<20 μs), large dynamic range (>22 dB) and low insertion loss (<0.3 dB).

References

1. Nigel Cockroft, "Array-based VOAs offer compact signal control", WDM solutions, Jun. 2001, p. 81.
2. D. Ostling and H.E. Engan, "Narrow-band acousto-optic tunable filtering in a two-mode fiber", Opt. Lett., vol. 20, no. 11, pp. 1247–1249, 1995.

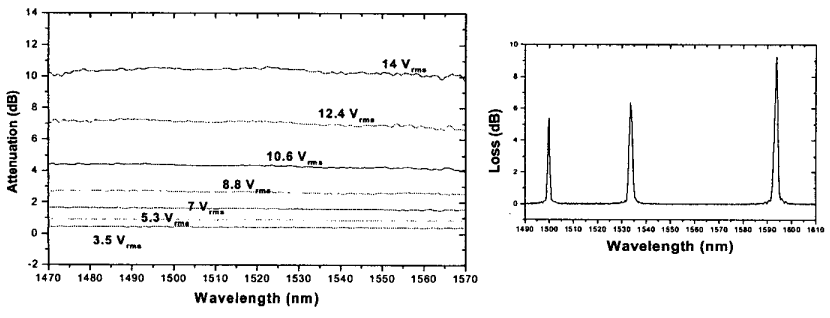

CMB5 Fig. 1. Attenuation spectrum of a 21-μm thick, 1.3 cm-long AOTF at different RF voltages. The corresponding filtering spectrum of an unetched, 30-cm long AOTF is also shown on the right for comparison.

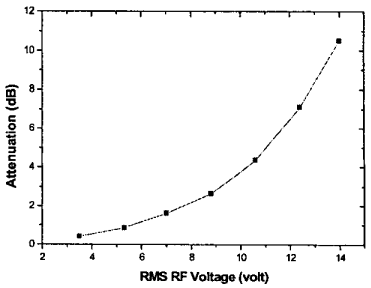

CMB5 Fig. 2. Attenuation versus RF voltage.

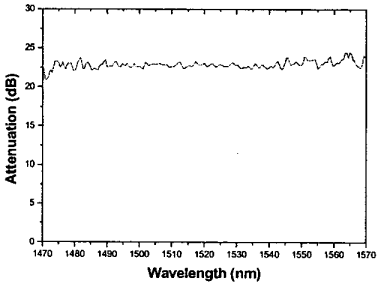

CMB5 Fig. 3. Attenuation spectrum of cascaded VOA.

3. Q. Li, X. Liu, J. Peng, B. Zhou and H.P. Lee, LEOS Proceeding 2001, ThV3.

CMB6 **9:15 am**

High Speed and High Power Performances of LTG-GaAs Based TWPDs In Telecommunication Wavelength (~1.3 μm)

Jin-Wei Shi and Yen-Hung Chen, Graduate Institute of Electro-Optical Engineering, National Taiwan University, Taipei 10617, Taiwan, Email: bd0122@ms17.hinet.net

Kian-Giap Gan, Yi-Jen Chiu, and John. E. Bowers, Department of Electrical and Computer Engineering, University of California, Santa Barbara, CA 93106.

Chi-Kuang Sun, Graduate Institute of Electro-Optical Engineering, National Taiwan University, Taipei 10617, Taiwan

Low-temperature-grown GaAs (LTG-GaAs) based photodetectors (PDs) merit a lot of attentions due to their short response time, high electrical bandwidth, high output saturation current, and low dark current. However the wide absorption band gap (~800 nm) of LTG-GaAs restricts its applications from long wavelength (1300 ~ 1550 nm) optical communications. Recently, several research groups had demonstrated LTG-GaAs based p-i-n, MSM PDs[1,2] in this wavelength regime by utilizing mid-gap defect state to conduction band transitions. However, these PDs usually suffered extremely low quantum efficiency (~0.6 mA/W)[2] or serious electrical bandwidth degradation due to long device absorption length for higher saturation power[1] and quantum efficiency purpose. In this paper, we demon-

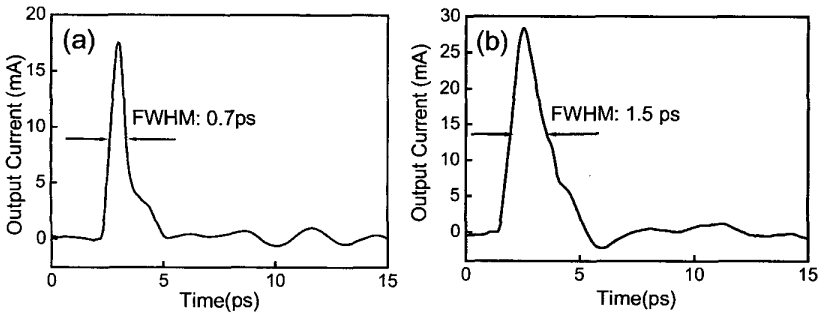

CMB6 Fig. 1. (a) shows Impulse response of a 10-μm-long LTG-GaAs p-i-n TWPD under 1230 nm excitation, and (b) shows Impulse response of a 40-μm-long LTG-GaAs p-i-n TWPD under 1230 nm excitation.

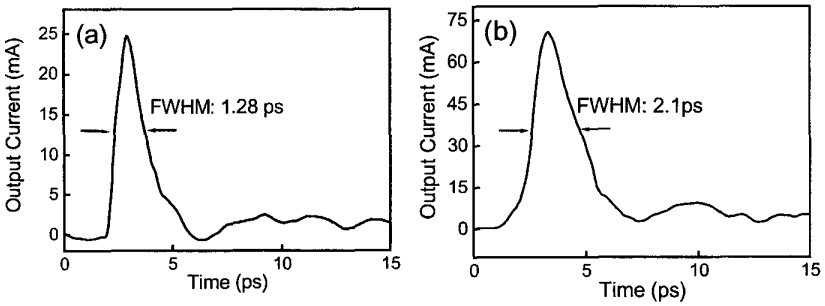

CMB6 Fig. 2. (a). Impulse response of a 70-μm-long LTG-GaAs MSM TWPD under 1230 nm excitation. (b) Impulse response of a 70-μm-long LTG-GaAs MSM TWPD under 1230 nm excitation with best peak-voltage-bandwidth product performance.

strated ultra-high speed and high saturation power performances of LTG-GaAs based MSM TWPD in the telecommunication wavelength regime (~1300 nm). Due to short carrier trapping time of LTG-GaAs layer and superior microwave guiding structure in MSM TWPD, record ultra-high peak power bandwidth product performance has been obtained in long absorption length devices.

The structures of measured p-i-n and MSM TWPDs are similar to previously reported ones.[1,3] We employed a femtosecond Cr^{4+}: forsterite laser operating at 1230 nm, which mimics the telecommunication wavelength of 1300–1550 nm, as the light source for transient electro-optical (EO) sampling measurements. Figure 1a shows an example of the measured impulse current response in a 10 μm-long LTG-GaAs based p-i-n TWPD. The measured EO trace showed an ultra-high speed performance with 0.7 ps FWHM. The measured response time is limited by carrier trapping time of LTG-GaAs photo-absorption layer. Its corresponding electrical bandwidth can be obtained by utilizing Fast Fourier Transform technique, which is about 280 GHz. The efficiency of measured p-i-n device is about 7 mA/W at 5 V bias. In order to increase the quantum efficiency and output saturation current, longer devices were also fabricated and measured. Figure 1b shows the measured impulse response of a 40 μm long p-i-n based TWPD. The response time FWHM is 1.5 ps, corresponding to a ~200 GHz electrical bandwidth with an efficiency of 11 mA/W at 5 V bias. In long absorption length devices, the response time is dominated by microwave loss and velocity mismatch of p-i-n based waveguide instead of carrier trapping time comparing with short absorption length devices.

With a superior microwave guiding structure in LTG-GaAs based MSM TWPD, even greater bandwidth and efficiency performances can be obtained. Figure 2(a) shows the measured impulse response of a 70μm-absorption-length LTG-GaAs MSM TWPD, which has a 1.28 ps response time corresponding to 234 GHz transformed electrical bandwidth. The efficiency of this measured MSM TWPD was further improved to ~13 mA/W at 18 V bias voltage. The ultra-high speed performance in long absorption length MSM TWPDs also implies its ultrahigh power-bandwidth-product performance. Under 28 pJ/pulse optical excitation energy, 160 GHz electrical bandwidth with 3.55 V peak output voltage was obtained under 10 V bias (figure 2b), corresponding to a record peak-output-voltage-bandwidth product of 568 GHz-V.[4] Figure 3 shows its corresponding frequency response. This ultrahigh power-bandwidth product performances of LTG-GaAs MSM TWPDs in telecommunication wavelength promise their applications in low-cost GaAs based photo-receiver circuits without electrical pre-amplifiers and high power photomixer devices which are compatible with fiber optical communication components.

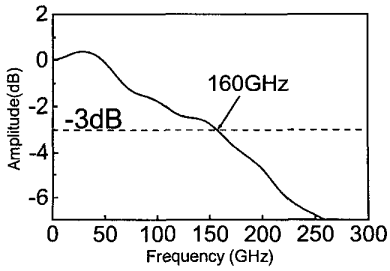

CMB6 Fig. 3. Frequency response of the impulse response trace in figure 2(b).

References

1. Y.J. Chiu, et al., *Electronics Letters*, **34**, 1253–1254, June (1998).
2. H. Erlig, *et al., Electronics Letters*, **35**, 173–174, Jan., (1999).
3. J.-W. Shi, *et al., IEEE Photon. Techno. Letters*, **16**, 623–625, June (2001).
4. K. Kato, *IEEE Trans. On Microwave Theory Tech.*, **47**, 1265–1281, Jul. (1999).

CMB7 **9:30 am**

Impact of Photodetector Nonlinearities on Photonic Analog-to-Digital Converters

P.W. Juodawlkis, J.J. Hargreaves, and J.C. Twichell, Lincoln Laboratory, Massachusetts Institute of Technology, Lexington, MA 02420, Email: juodawlkis@ll.mit.edu

1. Introduction

Photodetector nonlinearities can limit the performance of high-dynamic-range analog optical systems.[1,2] For systems that use short optical pulses to process or transmit analog information, this limitation is magnified due to the higher peak intensity at the photodetector input. In this paper, we examine the trade-off between signal-to-noise ratio (SNR) and linearity in optically sampled analog-to-digital converters (ADCs) due to saturation of the photodetector responsivity.

2. Measurement of photodetector nonlinear responsivity

The pulsed nonlinear response of a commercial InGaAs/InP p-i-n photodetector (7-GHz bandwidth, 50-μm diameter, 8-V bias) was characterized using 30-ps optical pulses generated by a mode-locked fiber ring laser (59.4-MHz rate, λ = 1550 nm) and amplified using an erbium-doped fiber amplifier (EDFA). The photodetector output current was measured using both a 50-GHz sampling scope and a DC current meter. The normalized data in Fig. 1 illustrate the pulse-width broadening and long tails that occur as the energy of the optical pulses increases. This pulse distortion results from reduced carrier velocity due to space-charge field screening.[3]

The integrated (R_{INT}) and peak (R_{PEAK}) nonlinear responsivity data (Fig. 2) reveal that pulse distortion occurs at significantly lower pulse energy E_P than the energy where the quantum efficiency decreases. The integrated responsivity is well described by the saturation expression

$$R_{INT}(E_P) = \frac{R_0}{1 + (E_P/E_{SAT})} \qquad (1)$$

where R_0 = 0.74 A/W is the linear responsivity, and E_{SAT} = 400 pJ is the saturation pulse energy. The excellent fit by Eq. (1) indicates that the source of the R_{INT} nonlinearity is saturation of the InGaAs absorbing material.[4]